공학석사학위논문

Characterization of Channelized Gas Reservoirs with an Aquifer Using EnKF and DCT

앙상블칼만필터와 이산코사인변환을 이용한
대수층 동반 가스채널저류층의 특성화

2016년 2월

서울대학교 대학원
에너지시스템공학부
이 충 호

Abstract

Reservoir characterization is estimation of reservoir properties and it is important for reliable predictions of future productions. The predictions help us make reasonable decisions. Ensemble Kalman filter (EnKF) is one of the powerful reservoir characterization methods, which allows reservoir properties to be updated in real time and provides uncertainty assessment on future productions.

EnKF has been applied to channelized reservoirs, but it has limitations of capturing channel patterns and connectivity. Especially, in channelized gas reservoirs with an aquifer, water influx increases uncertainty of gas behaviors. It is also difficult to estimate permeability distribution due to its bimodal distribution and complex connectivity. Thus, characterization of channelized gas reservoirs with an aquifer using EnKF has not been successful.

In this study, a new method using EnKF with discrete cosine transformation (DCT) and preservation of facies ratio (PFR) is proposed to characterize channelized gas reservoirs with an aquifer. The proposed method is compared with EnKF and EnKF with DCT. It shows the most reliable performances in estimating pattern and connectivity of the channels. Besides, this method predicts aquifer factors for the four sides with high reliability. Thus, it is obviously verified that the proposed method provides reliable future predictions of gas and water productions.

Keywords: ensemble Kalman filter (EnKF), discrete cosine transformation (DCT), preservation of facies ratio (PFR), channelized gas reservoirs, an aquifer factor

Student Number: 2014-20520

Table of Contents

List of Tables

List of Figures

1. Introduction

Reliable reservoir models are imperative for reasonable decision making such as production management and future development. It can be achieved by reservoir characterization, which is estimation of unknown reservoir properties by integration of available data into reservoir models. Since it provides proper prediction of future productions and uncertainty assessment, it is essential in petroleum engineering.

Ensemble Kalman filter (EnKF) is one of the most powerful reservoir characterization methods because it can be used to reflect new data in real time. Also, it is compatible with diverse forward models and types of static and dynamic data. Evensen (1994) introduced the method in ocean dynamics and Nævdal et al. (2002) utilized first for reservoir characterization in petroleum engineering.

Jeong et al. (2010) characterized reservoirs using gradual deformation method with EnKF. Jung and Choe (2012) proposed a streamline-assisted EnKF with covariance localization. Yeo et al. (2014) suggested covariance matrix localization using a drainage area in EnKF.

Contrast to non-channelized reservoirs, channelized reservoirs are difficult to be characterized due to its unique characteristics of channel connectivity and bimodal distribution of permeability. The pattern and connectivity of sand channels should be preserved to predict reservoir behaviors and future productions properly. To solve these problems, several researches have been conducted.

Shin et al. (2010) suggested non-parametric approach with EnKF for highly non-Gaussian permeability distribution in reservoirs. Nejadi et al. (2011) used entropy weighted EnKF for non-Gaussian permeability fields. Jafarpour and McLaughlin (2008) performed history matching with EnKF and discrete cosine parameterization to reduce size of reservoir states and

parameters. Lorentzen et al. (2012) proposed EnKF with level set function to preserve channel pattern. Lee et al. (2013a, 2013b) characterized channelized reservoirs using EnKF with a distance based method and clustering. Lee et al. (2014) suggested ensemble smoother with selective use of measurement data depending on water breakthrough to characterize channelized reservoirs.

Jafarpour and McLaughlin (2007) introduced discrete cosine transformation (DCT) in permeability parameterization for history matching of channelized reservoirs using EnKF. They proposed that DCT was a stronger parameterization alternative than Karhunen-Loeve transform (KLT), which was a conventional method to provide low-dimensional parameterization for history matching. Iterative least squares algorithm and EnKF were tested with DCT for history matching of channelized reservoirs (Jafarpour and McLaughlin, 2009). They suggested that DCT caught the spatial continuity of geological facies of channelized reservoirs.

Although many new methods related to channelized reservoirs have been studied, the previous researches primarily focused on oil reservoirs. Gas reservoirs with an aquifer have high uncertainty in productions and thus, they need to be characterized reliably like oil reservoirs. However, gas behaviors are different from those of oil. The main difference is higher mobility of gas than that of oil. Therefore, characterization of gas reservoirs should be achieved considering the characteristics of gas.

Gas reservoirs with depletion drive typically have 80~90% recovery factors. Also, heterogeneity of permeability affects less gas flow behaviors due to high gas mobility. Gas reservoirs without an aquifer have comparatively low necessity of reservoir characterization because of low uncertainty in gas productions and high gas recovery. However, an aquifer causes water fingering or gas trapping (Holtz, 2002). Therefore, gas reservoirs with water drive have much lower recovery factors of 50~70%,

depending on reservoir heterogeneity and aquifer strengths.

Figure 1.1 demonstrates the effect of an aquifer on uncertainty of gas productions. These are 100 channelized reservoir models and simulation conditions are identical except for aquifer properties. Figure 1.1a shows gas production rates at three wells of the 100 ensemble members without an aquifer. Figures 1.1b and 1.1c are those with aquifers of the four sides with the same and different strengths, respectively.

From Figure 1.1, there are three key points for channelized gas reservoirs. First, Figure 1.1a suggests that channelized gas reservoirs without an aquifer have low uncertainty in gas productions. Second, Figure 1.1b demonstrates increased uncertainty in gas productions compared to Figure 1.1a. As seen, the existence of the aquifer intensifies the uncertainty of gas productions. Third, Figure 1.1c indicates similar but slightly higher uncertainty of the gas productions due to different aquifer sizes. It means that different aquifer strengths of the four sides expand the uncertainty more.

In summary, water influx from an aquifer enlarges uncertainty in productions sharply. Thus, channelized gas reservoirs with an aquifer should be characterized for reliable prediction of future productions.

For gas reservoirs with an aquifer, water influx can be monitored by several different methods. Use of gravity data is possible because water gas displacement causes subsurface mass redistribution and it is detectable in a gravity survey. Hare et al. (1999) suggested that surface gravimetrical observations can indicate the progress of waterflooding. Stenvold et al. (2008) demonstrated that time-lapse gravimetrical data can locate water flooded areas and check gas displacement.

Glegola et al. (2012a, 2012b) characterized aquifer related factors for conventional gas reservoirs using EnKF. Kim et al. (2015) characterized gas reservoirs with an aquifer using only production data and considered different aquifer sizes at the four sides.

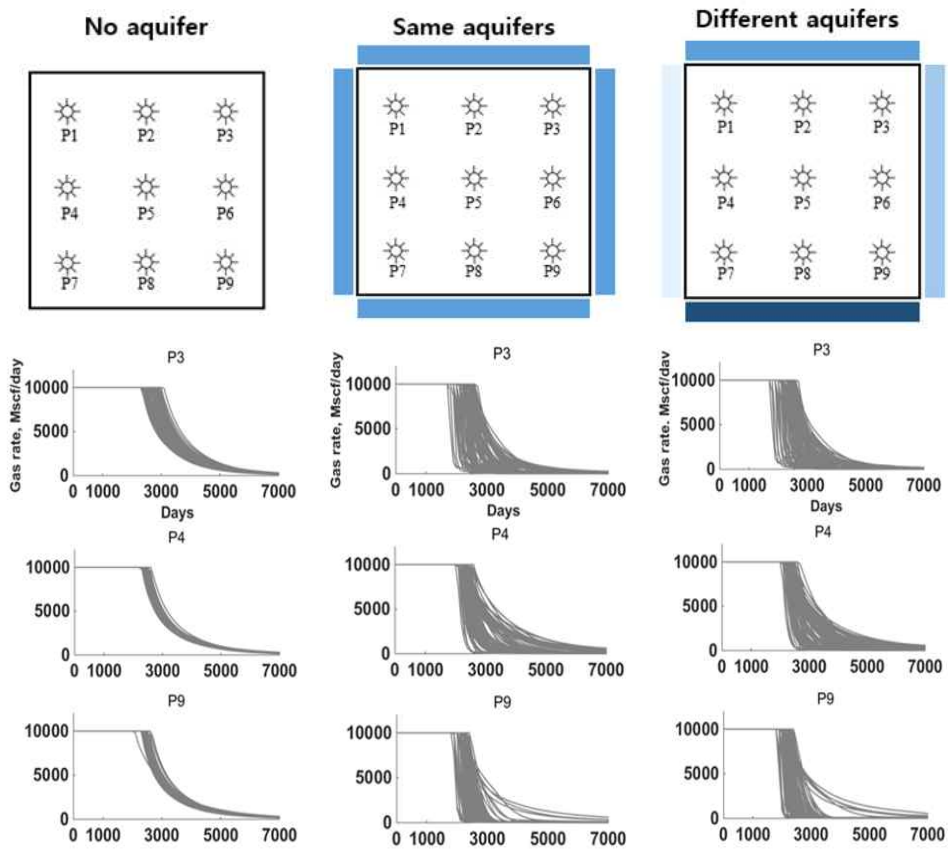

(a) (b) (c)

Figure 1.1 Gas production rates at P3, P4, P9 wells for 100 ensembles. (a) no aquifer, (b) aquifers of the same strengths at the four sides, and (c) aquifers of different strengths at the four sides.

Although the previous studies presented several methods to monitor or characterize an aquifer, none of them was applied to channelized gas reservoirs. Also, some of them require time-lapse 3D gravimetric data for practical aquifer characterization and the studies could not consider diverse aquifer sizes in a reservoir.

This paper presents characterization results of channelized gas reservoirs with an aquifer using static data and production data only without any other time-lapse data. Furthermore, different aquifer strengths and sizes at the four sides are considered for practical field applications.

2. Theoretical backgrounds

Reservoir rocks can store and transmit hydrocarbon fluids. In many cases, the reservoir rocks are sandstone or carbonates. There are four types of sandstones: dune sandstones, shoreline sandstones, river sandstones, and delta sandstones (Hyne, 2012).

The dune sandstone is created by wind in both desert and coastal environments (Figure 2.1a). One of its main characteristics is internal crossbeds (Figure 2.1b). Also, this rock consists of very well-sorted fine sand particles, so it can be a good reservoir rock (Hyne, 2012).

The shoreline sandstone is made in beaches, which are long and narrow deposits of well-sorted sand particles. Waves remove other particles such as silt and clay and develop the beaches into a long strip of sand. In Figure 2.2, during rising seas, beach sand can be deposited on an angular unconformity and form oil and gas reservoirs (Hyne, 2012).

The river sandstone is formed in a meandering river (Figure 2.3a). Sand is deposited inside of the meander and these deposited sand bars are called point bars (Figure 2.3b). The point bar sandstone can be a good oil and gas reservoirs (Hyne, 2012).

The delta sandstone is deposited by a river flowing into a body of water (Figure 2.4). Interaction between river deposition and wave erosion decides the structure of delta: constructive delta and destructive delta. Like other types of sandstone, the delta sandstone can be a good oil and gas reservoir (Hyne, 2012).

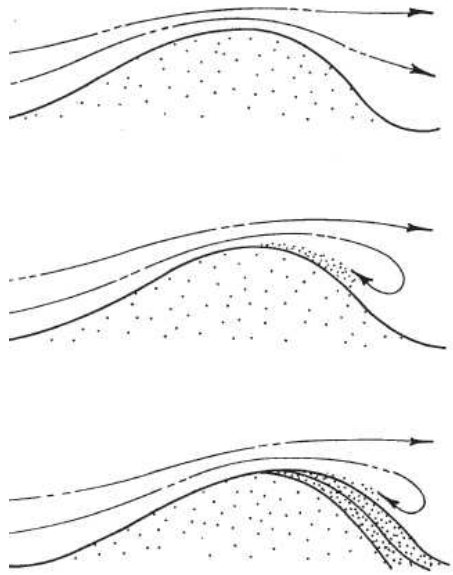

(a) Formation process

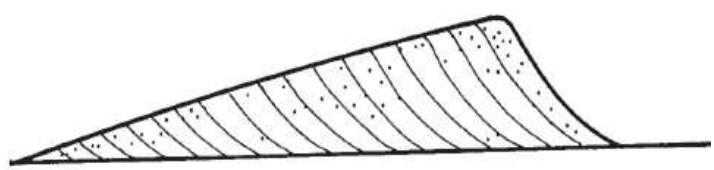

(b) Crossbeds in cross section

Figure 2.1 Sand dune (Hyne, 2012).

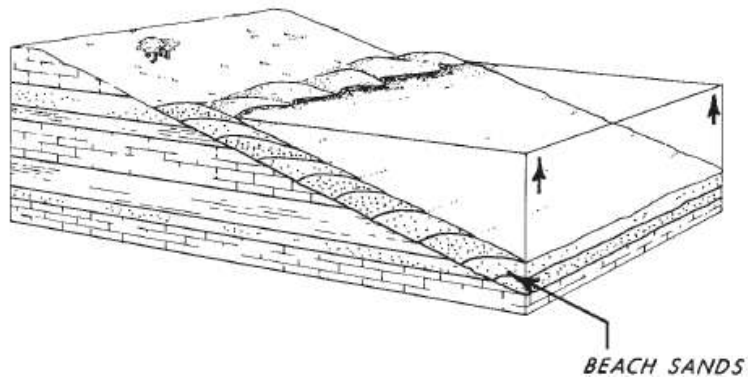

(a) Beach sands deposited by rising seas

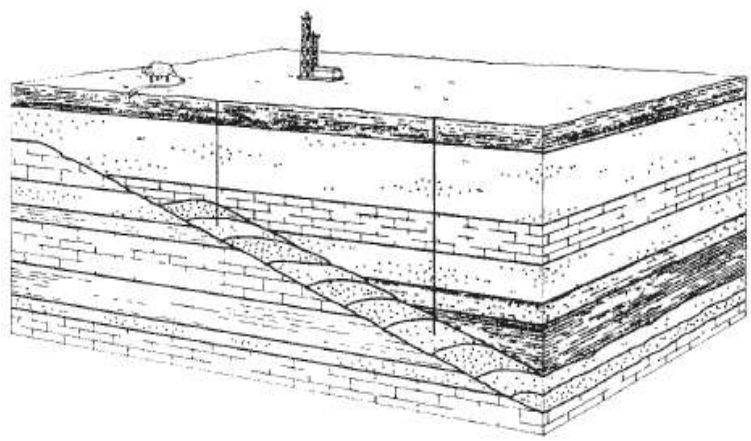

(b) Buttress sands created by beach sands

Figure 2.2 Beach sand (Hyne, 2012).

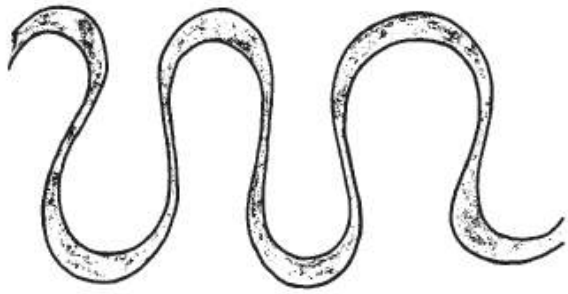

(a) Meandering river

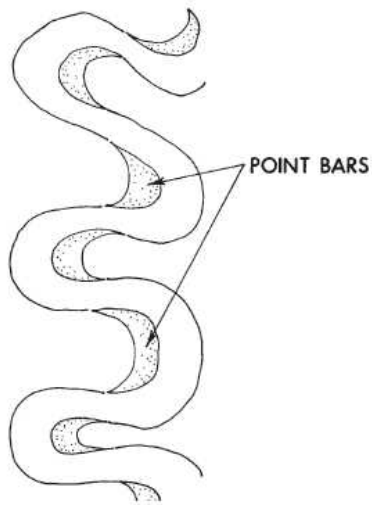

(b) Point bar sands

Figure 2.3 Depositing environment of river sandstone (Hyne, 2012).

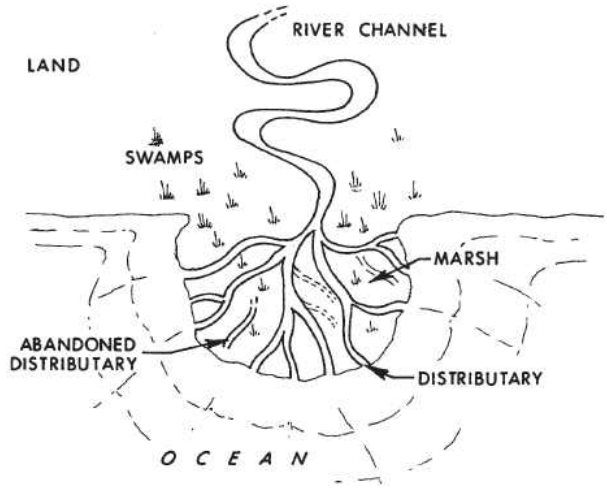

Figure 2.4 Depositing environment of delta sandstone (Hyne, 2012).

Most channel sandstones deposited in rivers are incised valley fills and a braided river constructs interconnected channels (Figure 2.5). In delta structures, rivers can divide into several channels called distributaries. Channelized reservoirs formed by these sandstone channels have their own unique patterns and connectivity (Figure 2.6).

The pattern and connectivity of channels affect oil, gas, and water productions highly. However, these properties are typically difficult to be predicted reliably in channelized reservoirs. The reservoirs show high heterogeneity and a bimodal distribution in permeability values. This makes history matching of channelized reservoirs using EnKF present unreliable results (Lee, 2014).

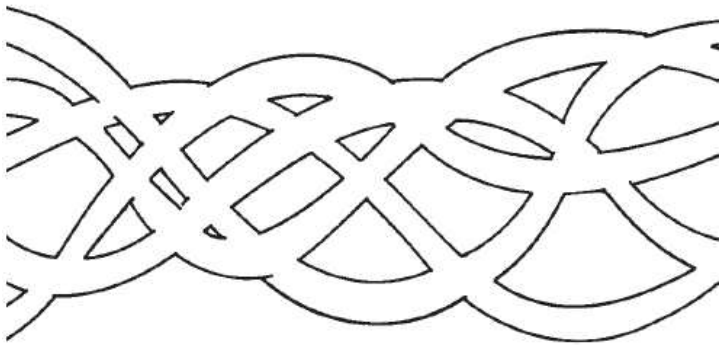

Figure 2.5 Braided river (Hyne, 2012).

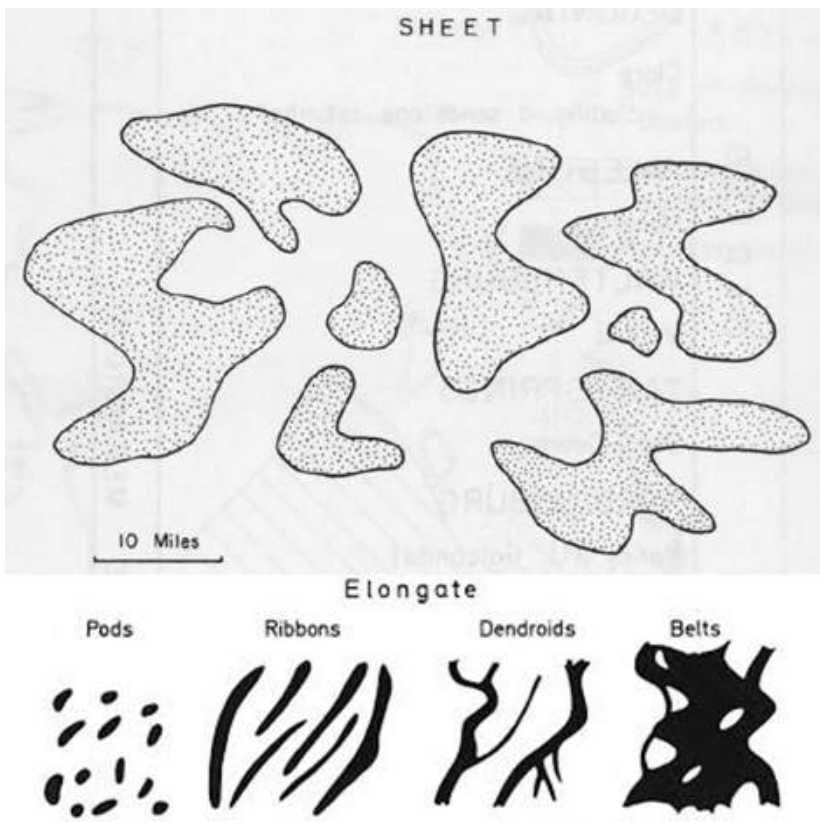

Figure 2.6 Horizontal connectivity of sand channelized reservoirs (Potter, 1962).

3. Methodologies

3.1 Ensemble Kalman filter

In EnKF, a state vector means one realization of all parameters of interest, which are composed of static data, dynamic data, and observed data as Equation 3.1.

$$y_{t,i} = \begin{bmatrix} m_t^s \\ m_t^d \\ d_t \end{bmatrix} \tag{3.1}$$

where, $y_{t,i}$ is the state vector of the i-th realization at time t. m^s, m^d, and d correspond to the static data, dynamic data, and observed data, respectively.

EnKF has two steps. One is forecast step and the other is assimilation step. In the forecast step, a forward simulator predicts future dynamic behaviors using present static and dynamic data as Equation 3.2. In the assimilation step, the state vectors are assimilated by Equation 3.3 using Kalman gain (K) in Equation 3.4, which comes from minimizing the estimate error covariance (C_Y), Equation 3.5. When the predicted data and the observed data are quite different, the state vectors tend to be modified greatly.

$$\begin{bmatrix} m_{t+1}^d \\ d_{t+1} \end{bmatrix} = f(m_t^s, m_t^d) \tag{3.2}$$

$$y_j^a = y_j^p + K(d_j - Hy_j^p) \tag{3.3}$$

$$K = C_Y^P H^T (HC_Y^P H^T + C_D)^{-1} \tag{3.4}$$

$$C_Y^P = \left(\frac{1}{N_e - 1}\right) \sum_{i=1,j=1}^{N_e} (y_i^p - \overline{y^p})(y_j^p - \overline{y^p})^T \tag{3.5}$$

where, superscripts a and p mean assimilated and priori, respectively; d_j represents the observed data, which are regarded as true; Hy_j^p is the predicted dynamic data; H and C_D are the measurement operator and the observation error covariance, respectively; N_e is the number of ensembles; $\overline{y}$ means the average of all ensemble members, which is considered as the true state vector.

3.2 Discrete cosine transformation

DCT is one of parameterization methods for data compression. It uses real cosine functions as transformation kernels. One dimensional (1D) DCT is like Equation 3.6 and inverse DCT is given by Equation 3.7.

$$v(k) = \alpha(k) \sum_{n=0}^{N-1} u(n) \cos\left[\frac{\pi(2n+1)k}{2N} \right], 0 \le k \le N-1 \quad (3.6)$$

where, $\alpha(k) = \begin{cases} \sqrt{2/N} & k = 0 \\ \sqrt{1/N} & 1 \le k \le N-1 \end{cases}$.

$$u(n) = \sum_{k=0}^{N-1} \alpha(k) v(k) \cos[\frac{\pi(2n+1)k}{2N}], 0 \le n \le N-1 \quad (3.7)$$

where, u(n) is the signal and N is the length of the signal u(n).

In a two-dimensional image, DCT basis functions are organized in a descending order from the upper-left to the lower-right corresponding to their level of detail and representation of trends. In Figure 3.1, we can confirm the property. Basis functions at the upper-left corner represent overall trend with low level of detail. The bases at the lower part of the corresponding matrix show vertical connectivity and those at the right part mean horizontal connectivity.

One variable value in a grid is expressed by the sum of M cosine basis functions. A set of M DCT-weighting coefficients illustrate one image. When N is the number of grids of an image and M equals N, the image can be recreated perfectly by the coefficients. If M<N, some features of the

image will be lost. However, the compressed DCT representation of the image is compact and still shows overall characteristics of it.

Figure 3.2a describes an example image and Figure 3.2b is logarithms (log) of DCT coefficients matrix of the image. We can see that the values at the upper-left part are large compared to other values. Figure 3.3 illustrates some representations of the example image using small part of the whole DCT coefficients. The image made by only 10% of the whole DCT elements reflects the overall trend and pattern of the original image (Figure 3.3c).

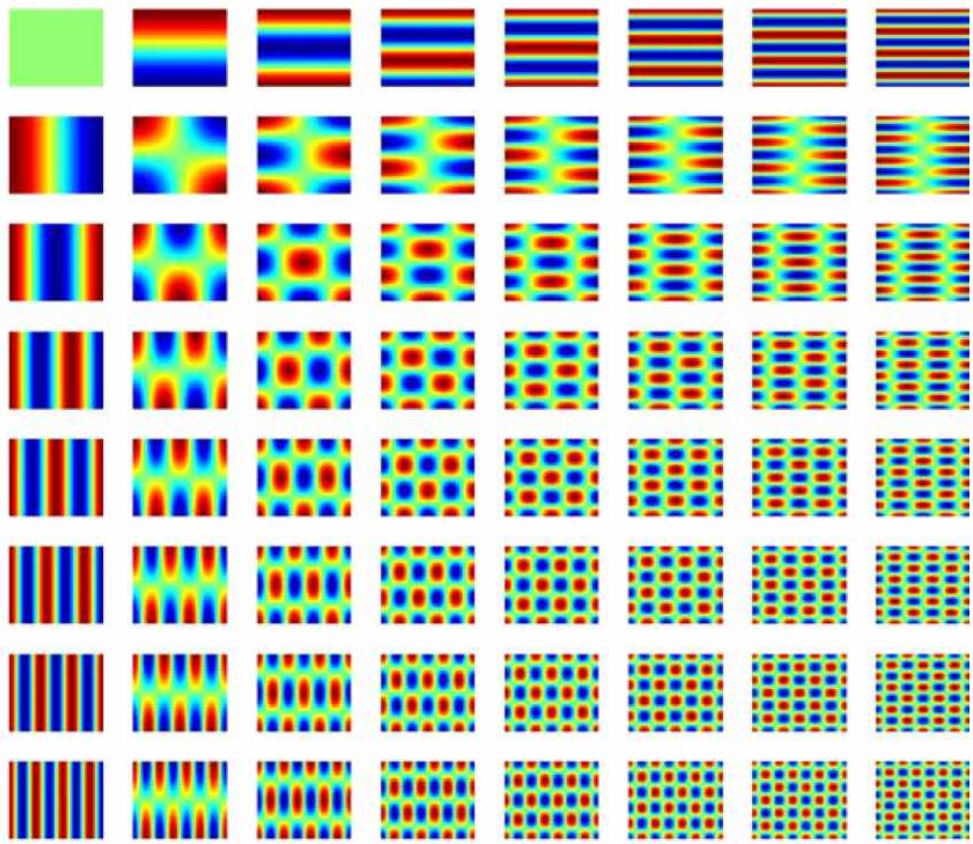

Figure 3.1 Low-frequency DCT bases (Jafarpour and McLaughlin, 2007).

(a) Original image (576 by 576)

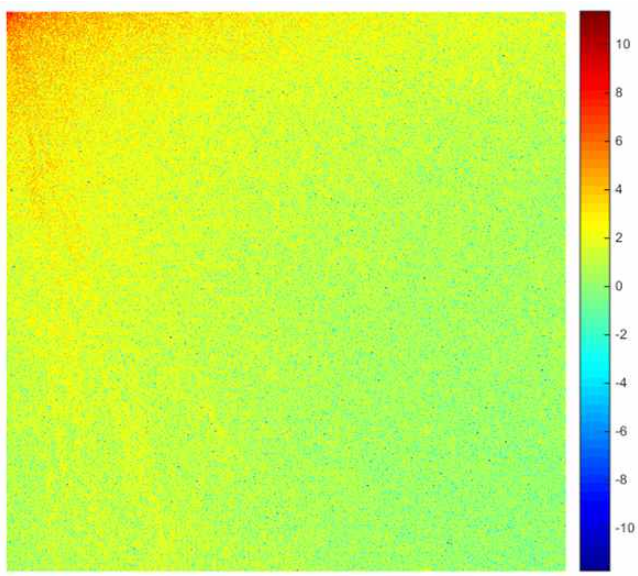

(b) Log-DCT coefficients

Figure 3.2 An example image and log values of DCT coefficients.

(a) 1% of whole DCT elements

(b) 5% of DCT elements

(c) 10% of DCT elements

Figure 3.3 Low-rank representations of the example image using different numbers of DCT elements.

DCT can be condensed by a set of linear equations. The forward transformation from N grid values to the M coefficients is given by Equation 3.8. The inverse problem can be solved using the M DCT-weighting coefficients of the basis functions like Equation 3.9.

$$v_t = Au_t \tag{3.8}$$

$$u_t = A^T v_t \tag{3.9}$$

where, u_t means the N grid block values and v_t represents the M DCT-weighting coefficients; A^T is N by M unitary matrix with M basis vector columns.

In history matching, DCT has advantages over KLT. DCT is faster and requires fewer assumptions than KLT, while as accurate as KLT. It is more computationally efficient using Fast Fourier Transform than KLT, which needs singular value decomposition. Since its basis vectors are predetermined and data-independent, they can be calculated and stored just once (Jafarpour and McLaughlin 2007, 2008, 2009).

A 2D log permeability field, which has N by N grids, is transformed into N by N DCT coefficients value matrix. DCT estimation of the field is a linear combination of a specific number of predefined basis functions. A part of the DCT basis images can express major channel pattern of the original field.

A small fraction of the largest DCT coefficients, which are gathered in the upper-left corner of the matrix, will be used to represent the permeability field. The coefficients are set as elements of a state vector in EnKF. After the assimilation in the procedure of EnKF, assimilated DCT coefficients are utilized in the inverse procedure, which creates an

assimilated log permeability field.

Figure 3.4 demonstrates effects of the number of DCT elements, which are applied in the inverse problem. The property of the representation using parts of the whole DCT elements works equally in channelized reservoirs like the example image, e.g. Figure 3.3. Dimension of the reference log permeability field is 39 by 39.

Figure 3.4a is the reference field in this study, which consists of 1,521 grids. It also means the field, which comes from the inverse procedure utilizing the whole DCT elements. Figure 3.4b is an estimated field from the DCT inverse process using 66 upper-left DCT coefficients, 4.3% of the total. Figures 3.4c and 3.4d are derived from 120 and 190 upper-left DCT elements, respectively. It confirms that only a small part of the whole DCT elements is enough to capture the trend of the original field with keeping their channel pattern.

In this study, DCT is used not to increase precision in estimating channel properties but to catch primary pattern of the channels. Additionally, DCT saves memory usage and decreases simulation times.

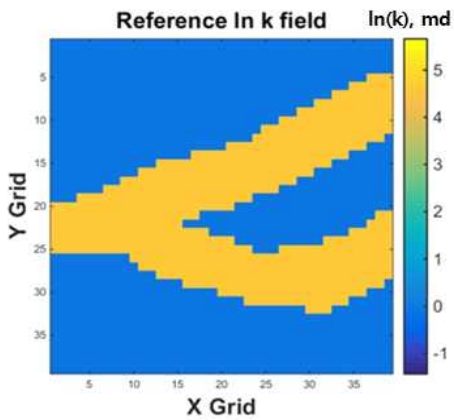

(a) 1521 DCT elements

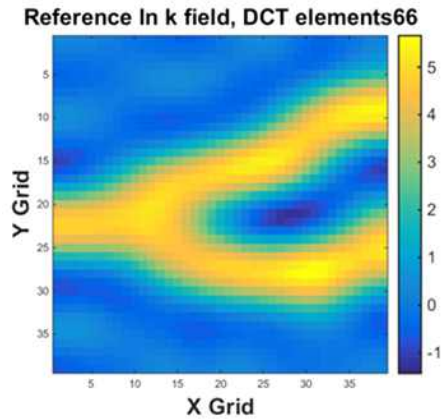

(b) 66 DCT elements

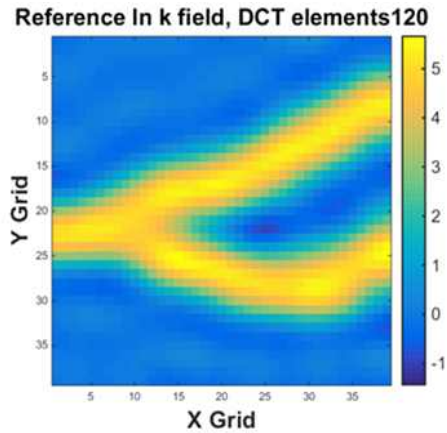

(c) 120 DCT elements

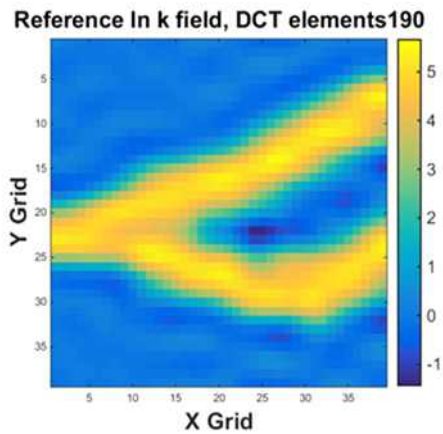

(d) 190 DCT elements

Figure 3.4 Transformed log permeability fields of the reference reservoir by the inverse DCT with various number of DCT coefficients. (All 1,521 DCT elements are required for perfect inversion.)

3.3 Preservation of facies ratio

Rock facies is a distinctive rock type of the rock layer. In channelized reservoirs, distribution of the facies is very important because productivity highly depends on the type of facies such as sandstone or shale. From geological survey, we can get overall facies ratio of the interested area.

In this paper, a method to preserve facies ratio is utilized to convert the assimilated permeability field. Permeability values of the whole grids in the field are sorted by the descending order. Based on the facies ratio known, the upper part of the whole values is changed to sand of 100 md and the rest is transformed into shale of 1 md.

This modification is reasonable because it is based on the fact that a grid with a high permeability value has high probability to be sand. The sandstone facies ratio of the reference is 0.34 and the ratio is applied to PFR. Figure 3.5 shows impacts of the PFR on the log permeability field. Figure 3.5a is one assimilated ensemble member and Figure 3.5b represents the same ensemble transformed by PFR.

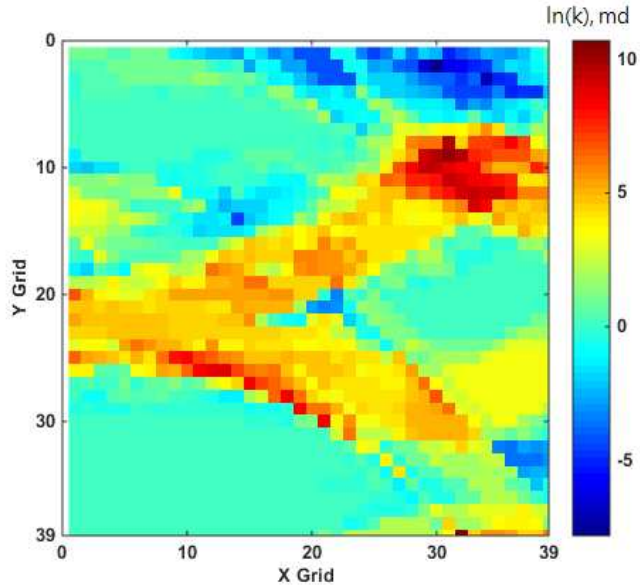

(a) An assimilated ensemble

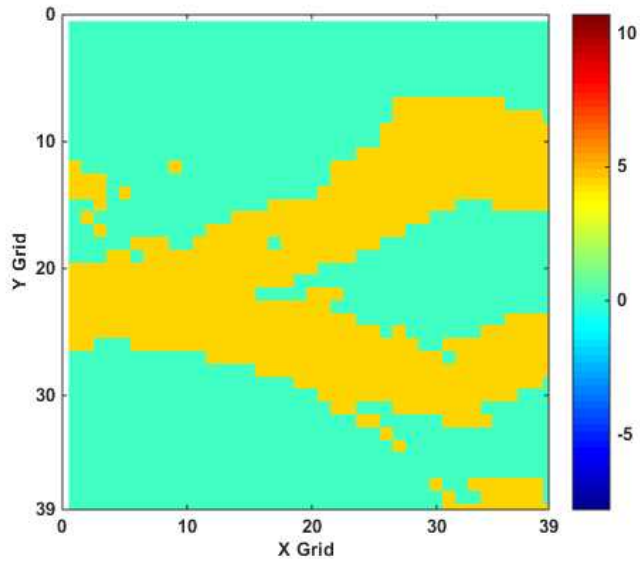

(b) A PFR applied ensemble

Figure 3.5 Assimilated log permeability fields without and with PFR.

3.4 Reservoir characterization using EnKF, DCT, and PFR

In this study, reservoir characterization is achieved by three methods: EnKF alone, EnKF with DCT, and EnKF with DCT and PFR. They will be compared in terms of the performances of figuring out the principal trend of channel and preserving channel properties. Also, in accordance with the estimation of channel, productions will be predicted.

In Figure 3.6, the procedure of conventional EnKF is presented by the black boxes. Initial ensembles of channelized reservoirs are generated by geostatistical methods. The methods use information of facies on gas wells and channel pattern of the area of interest. The ensembles are simulated by a forward simulator. State vectors are updated by calculated Kalman gain. Forward simulation using the assimilated ensembles and update are repeated. After the last update, we can get final assimilated ensembles.

In EnKF with DCT, DCT is utilized to capture channel pattern efficiently. DCT and inverse DCT are added to the standard procedure of EnKF. From Figure 3.6, the black and red boxes represent the process of EnKF with DCT. Instead of log permeability, transformed log permeability by DCT is used. After the assimilation, the transformed permeability is converted into log permeability by solving DCT inverse problem.

In EnKF with DCT and PFR, PFR as an assistant scheme to DCT is applied to preserve channel properties such as two types of facies and connectivity. Three additional processes are added to the standard procedure of EnKF: DCT, inverse DCT, and PFR.

Figure 3.6 describes the procedure of the proposed method. Red and blue boxes illustrates DCT and PFR applications, respectively. Overall processes are similar to EnKF with DCT, but the transformed permeability by the inverse DCT is modified by PFR. PFR assigns sand or shale to whole grids of assimilated ensembles. By PFR application, the updated ensemble

members are transformed into channelized reservoirs with a bimodal distribution.

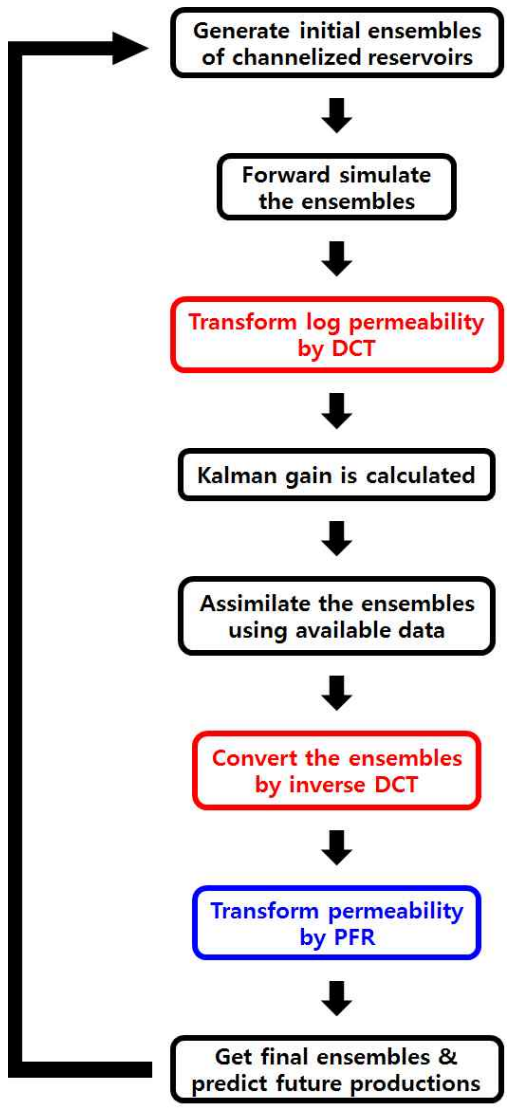

Figure 3.6 Overall procedures of EnKF with DCT and PFR. (The red and blue boxes show DCT and PFR applications, respectively.)

4. Results

4.1 Ensemble generation and simulation conditions

In this research, synthetic channelized gas reservoirs are history matched. Grid system is 39 by 39. Size of a grid cell is 250, 250, and 100 ft of x, y, and z axis, respectively. The reference and 100 initial ensembles are generated by SNESim (Single Normal Equation Simulation) using SGeMS. Figure 4.1a shows TI (Training Image) used and Figure 4.1b presents nine known data as facies indicators in the generation step. Figure 4.1c displays four log permeability field samples of the initial ensembles. Table 4.1 shows the conditions in TI generation and Table 4.2 lists simulation conditions.

There are nine production wells (Figure 4.1b). Gas production rate and BHP (bottomhole pressure) limit are 10000 Mscf/day and 1000 psia at all wells, respectively. MULTPV keyword of ECLIPSE 100, which means how much pore volume of a grid is multiplied, is utilized for aquifer modeling. Multiplying pore volume of the grids, which are saturated 100% by water, represents an aquifer. MULTPV value signifies strength and size of an aquifer simultaneously.

Intrinsic uncertainty of the aquifer in strength is considered by different MULTPV values at the four sides. The values come from the uniform distribution between 40 and 65. This distribution is adopted by the fact that aquifer volume is four to seven times as large as the pore volume of the reservoir. In the reference reservoir model, the East aquifer is strong, the North aquifer is moderate, and the rest are weak.

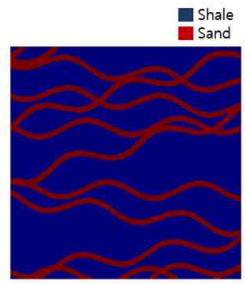

(a) Training image

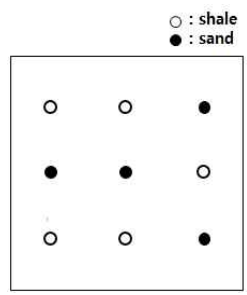

(b) Known data at the 9 wells

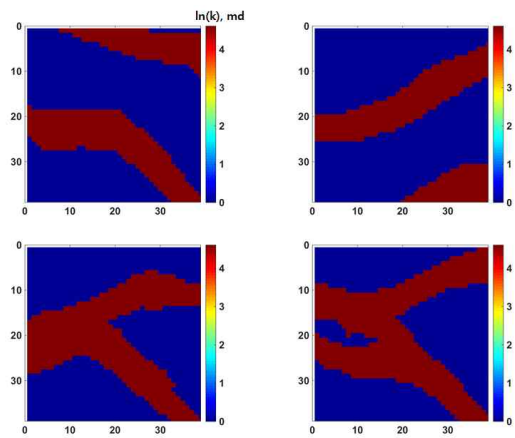

(c) Log permeability fields of four sample realizations generated by SNESim

Figure 4.1 Basic information of the reservoir of interest and initial ensembles using the information.

Table 4.1 Conditions in TI generation

Properties	Values
Grid system	[300 by 300 by 1]
Sizes of grid cell, ft	250, 250, 100
Number of facies types	2
Geobody type	Sinusoid
Facies ratio, fraction	0.2 (sandstone), 0.8 (shale)
Width, cell	7
Orientation, degree	Uniform distribution (70 ~ 110°)
Amplitude, cell	10
Wavelength, cell	120

Table 4.2 Simulation and reservoir conditions

Properties	Values
Reservoir type	Dry gas
Well location, grid coordinate	(8, 8), (20, 8), (32, 8), (8, 20), (20, 20), (32, 20), (8, 32), (20, 32), (32, 32)
Assimilation time, days	500, 1000, 1500, 2000, 2500
Total simulation period, days	7000
Observed data types	Well gas production rate, Well bottomhole pressure
Porosity, fraction	0.15
Initial water saturation, fraction	0.25
Initial reservoir pressure, psia	3000
Number of used DCT elements	120

The state vectors are composed of log permeability, MULTPV values, gas production rates, and BHPs. Permeability and MULTPV are static data. Gas rates and BHPs are observed data. Total simulation time is 7,000 days and observations are implemented for 2,500 days with 500 days interval.

Each assimilation updates permeability and MULTPVs. Then, we can obtain predictions of gas and water production rates of each well and total gas and water productions as a result. Figures 4.2 to 4.9 present results by the three methods compared with the reference performances.

4.2 Gas and water production rates

Figures 4.2 and 4.3 show gas and water production rates of the nine wells. The grey lines are rates of the 100 ensembles. The blue lines represent the averages of the rates and the red lines imply rates of the reference.

Wells 3, 4, 5, and 9 maintain the plateau gas production for about 3,000 days, while the others keep the plateau for a short time and start to decrease. In wells 3, 4, and 9, water breakthrough occurs during the simulation time due to their high permeability in near-wellbore region. The facies at each well position result in this tendency. The productive wells are placed at high permeable facies and the non-productive wells are located at low permeable facies (note Figure 4.1b).

Figures 4.2d and 4.3d present results of 100 assimilated ensembles by the proposed method. The bands of gas rates of productive wells cover rates of the reference and the means of the rates correspond with the true trend lines. Although the proposed method provides better characterization results than the other two methods, we need to check other performances in detail.

For gas and water production rates of the 100 initial ensembles (Figures 4.2a and 4.3a), the non-productive wells show small uncertainty due to very low production rates. However, the productive wells display high uncertainty with a wide bandwidth. As expected, the averages of the rates cannot predict the true rates of the wells and the times for water breakthrough are estimated poorly.

For the conventional EnKF (Figures 4.2b and 4.3b) and the EnKF with DCT (Figures 4.2c and 4.3c), uncertainties in the rates of all wells are reduced after the updates. The averages of the rates of the whole wells and the true rates are matched fairly. However, in some cases by the EnKF with DCT, though water breakthrough does not happen at wells 4 and 9, the results present water breakthrough at the wells.

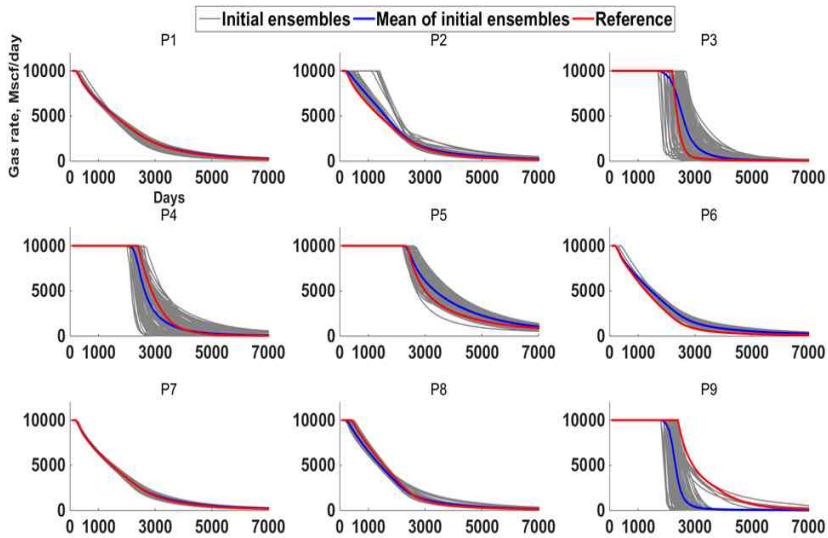

(a) Initial ensembles

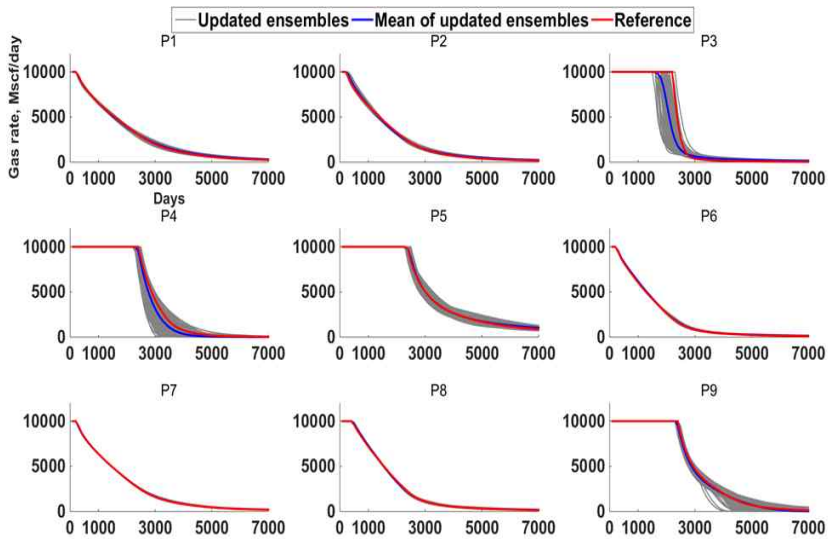

(b) EnKF alone

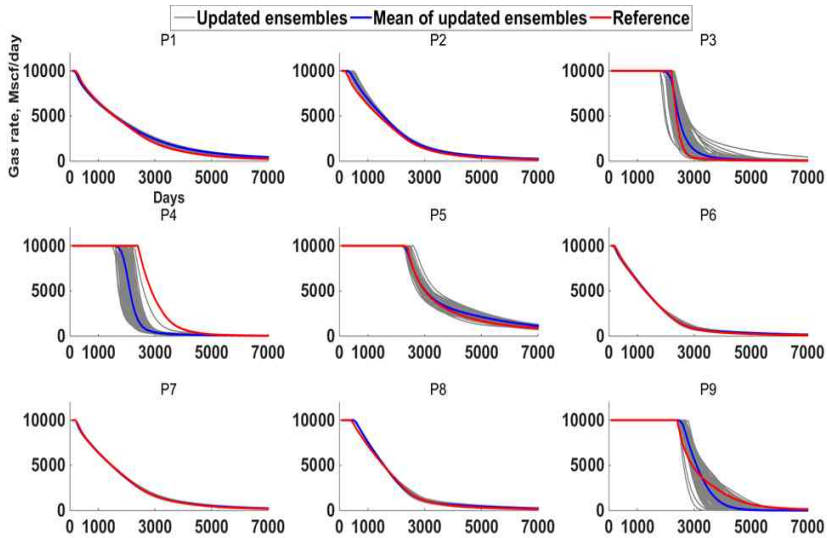

(c) EnKF with DCT

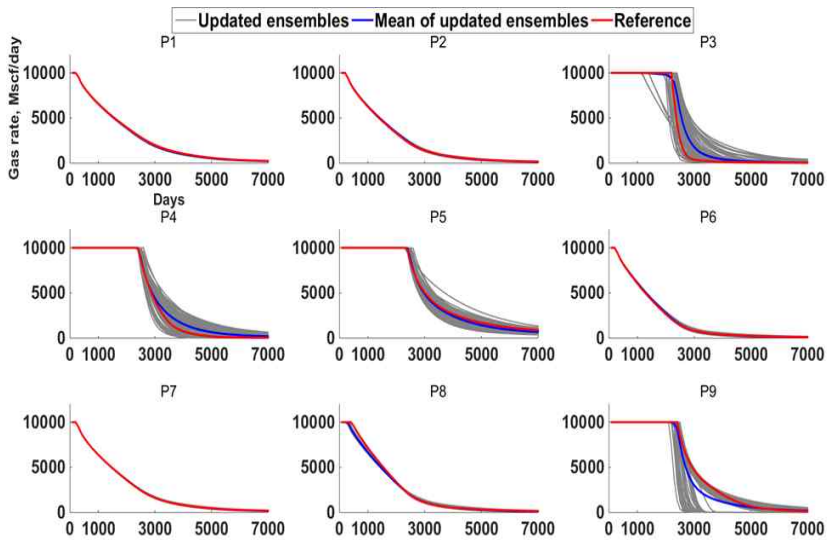

(d) EnKF with DCT and PFR (the proposed method)

Figure 4.2 Gas rate predictions of the initial and updated ensemble models.

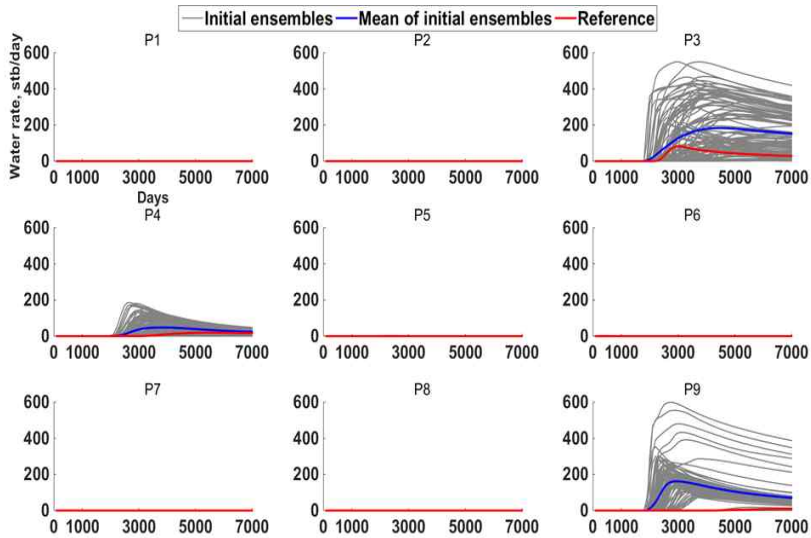

(a) Initial ensembles

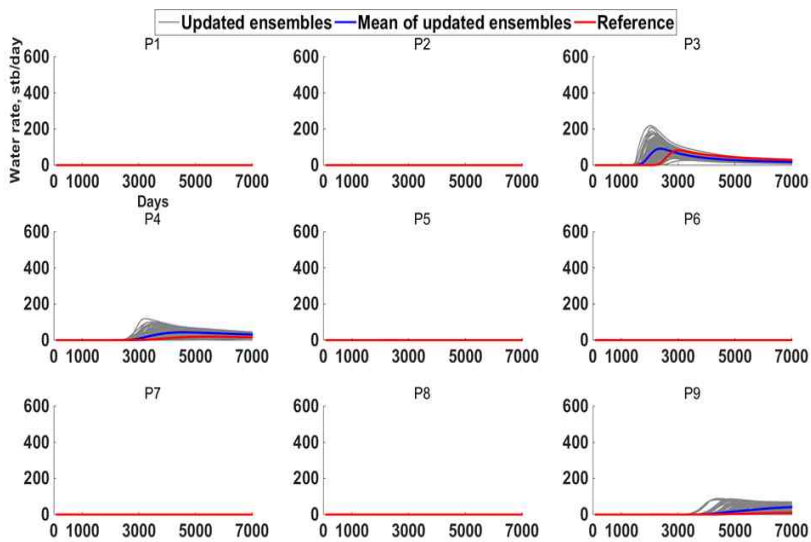

(b) EnKF alone

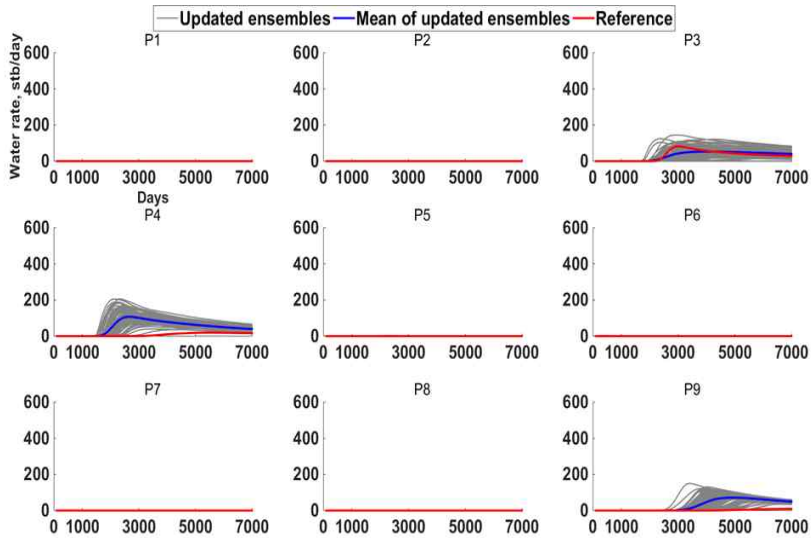

(c) EnKF with DCT

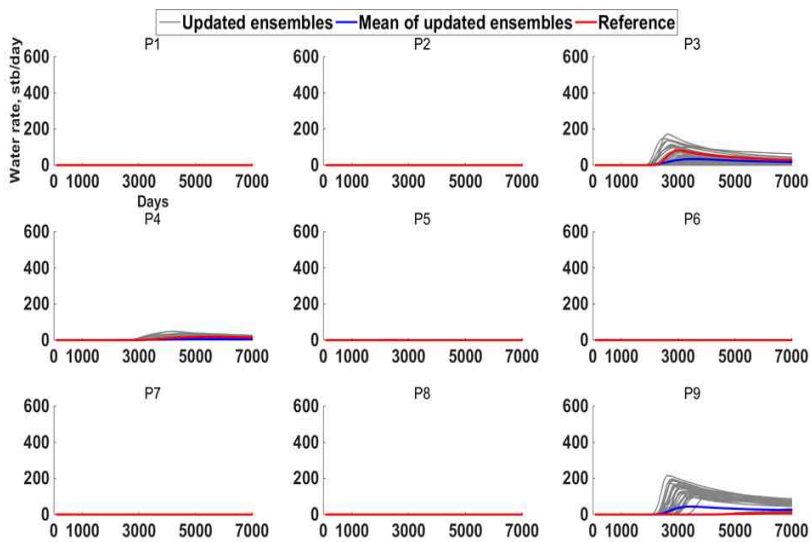

(d) EnKF with DCT and PFR (the proposed method)

Figure 4.3 Water rate predictions of the initial and updated ensemble models.

4.3 Total gas and water productions

Figures 4.4 and 4.5 are total gas and water productions of the initial and assimilated ensembles, respectively. The total gas production has comparatively low uncertainty meaning that gas production in each ensemble is similar due to simple behaviors of gas flow. High mobility of gas mitigates effects of permeability heterogeneity on gas flow.

On the contrary, water production indicates high uncertainty because water flow is highly affected by permeability distribution (Kim et al., 2015). For the initial ensembles (Figures 4.4a and 4.5a), water production reveals wide bandwidth and the means of the gas and water productions cannot match the true lines, respectively. The prediction overestimates total water productions.

For the conventional EnKF (Figures 4.4b and 4.5b), the uncertainty in gas and water productions is decreased greatly due to the updates and the mean of the water productions is similar to the true production of the reference field. However, the prediction of gas productions underestimates the true gas production. For the EnKF with DCT (Figures 4.4c and 4.5c), the means of the gas and water productions cannot predict the true lines properly.

Figures 4.4d and 4.5d present a case by the proposed method. The uncertainty in gas and water productions is lowered and the means of the predicted productions match up with the true productions properly even better than the conventional EnKF.

Figure 4.6 displays total water productions of each case at the final time step in box plots. The first and third quartiles cover the true value (green dotted line) only in the case of the proposed method. The others overestimate the water productions.

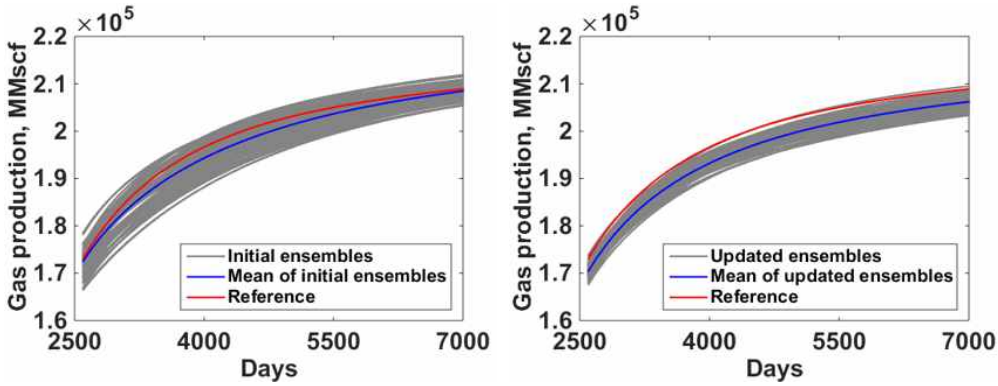

(a) Initial ensembles (b) EnKF alone

(c) EnKF with DCT (d) The proposed method

Figure 4.4 Total gas productions predicted by the initial and updated ensemble models.

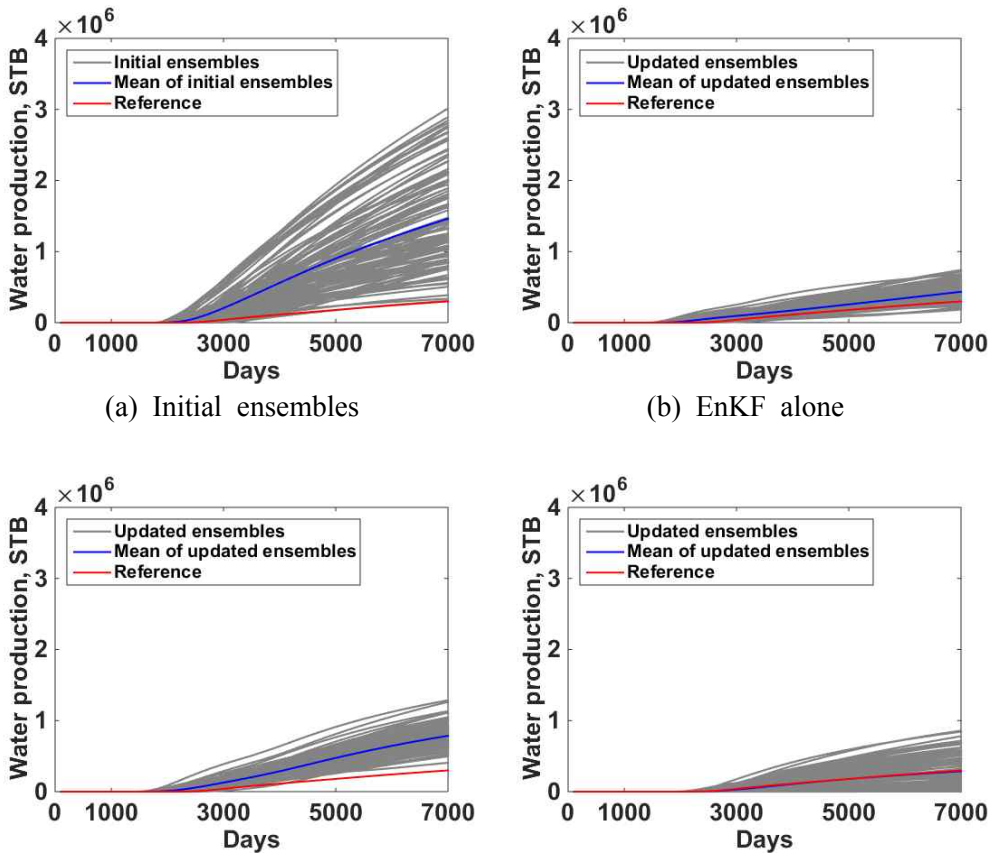

(a) Initial ensembles (b) EnKF alone

(c) EnKF with DCT (d) The proposed method

Figure 4.5 Total water productions predicted by the initial and updated ensemble models.

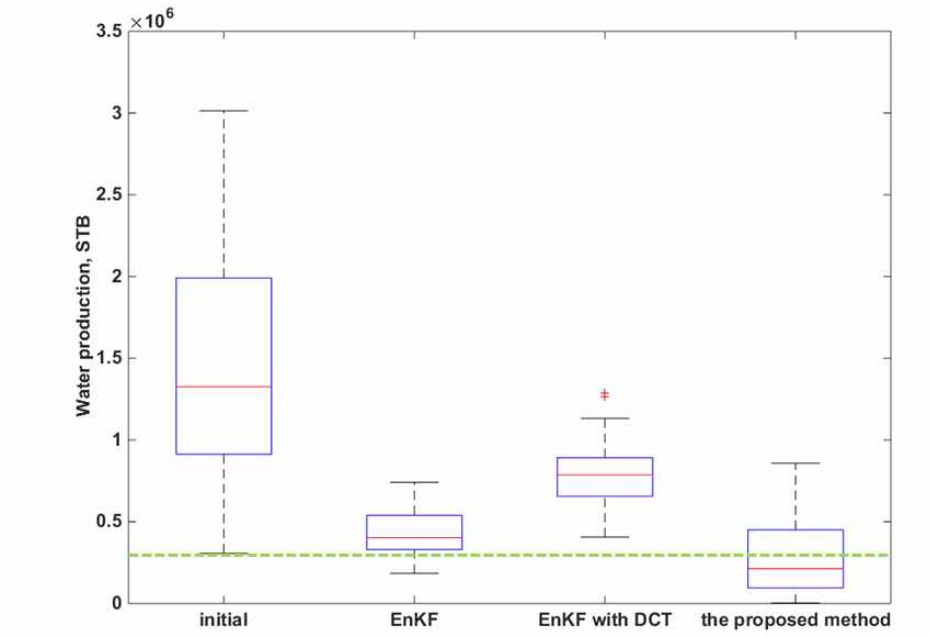

Figure 4.6 Box plot of total water productions at 7000 days by the initial and updated ensembles.

4.4 Pattern and connectivity of channels

Figure 4.7 shows log permeability distributions of the reference, initial, and assimilated ensembles with their histograms. Figure 4.8 represents three examples of the initial ensembles and their updated ensembles by the three methods. As expected, the average of the initial ensembles (Figure 4.7b) cannot represent the reference (Figure 4.7a) due to geostatistical generations using limited data. Major pattern and its frequency of the channels are quite different from those of the reference.

Although the conventional EnKF (Figures 4.7c and 4.8b) presents overall trend of the reference, it shows over-/under-shooting problem, which is also noticeable from its histogram, and cannot provide proper connectivity. Results from the EnKF with DCT (Figures 4.7d and 4.8c) show poor connectivity, gradation of permeability, and overshooting issues. Both the EnKF and the EnKF with DCT do not reflect the bimodal distribution due to the tendency of EnKF for becoming a normal distribution.

However, the proposed method (Figures 4.7e and 4.8d) manages the pattern and connectivity of the reference without overshooting problem. It also maintains the bimodal distribution and the highest and lowest values of the histogram are retained like the reference. This means that the pattern and connectivity of channel of the reference are well preserved using PFR.

Table 4.3 shows values of root-mean-square error (RMSE) of means of updated ensembles in log-permeability scale. The average of ensembles assimilated by the proposed method presents the lowest RMSE value at 1.537. Therefore, by the proposed method, geometrical properties of the channels of the reference are estimated properly.

Unlike channelized oil reservoirs, characterization of channelized gas reservoirs needs PFR additionally. This results from a fact that gas flow is highly affected by pressure differential rather than permeability in

comparison with oil. Assimilation from the gas rates only cannot reflect permeability distribution reliably. It causes ill-posed problem in characterization of gas reservoirs. Thus, additional methods like PFR are essential in characterization of channelized gas reservoirs to reduce the above problem.

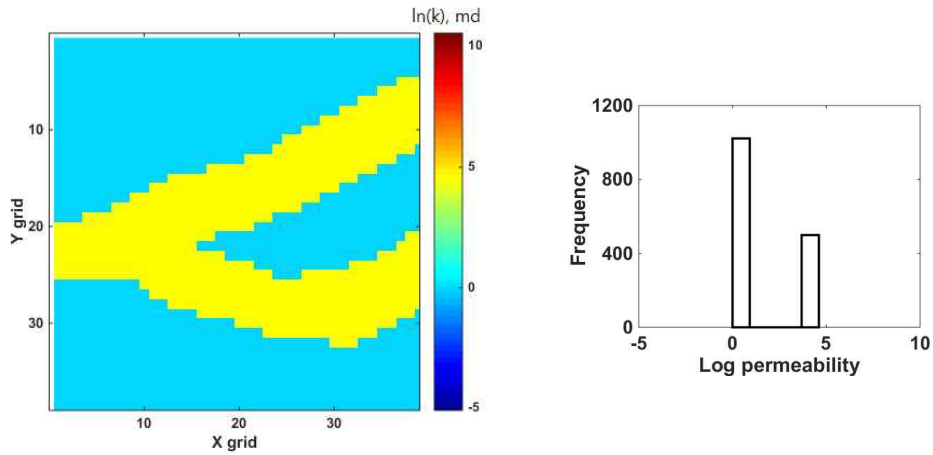

(a) The reference

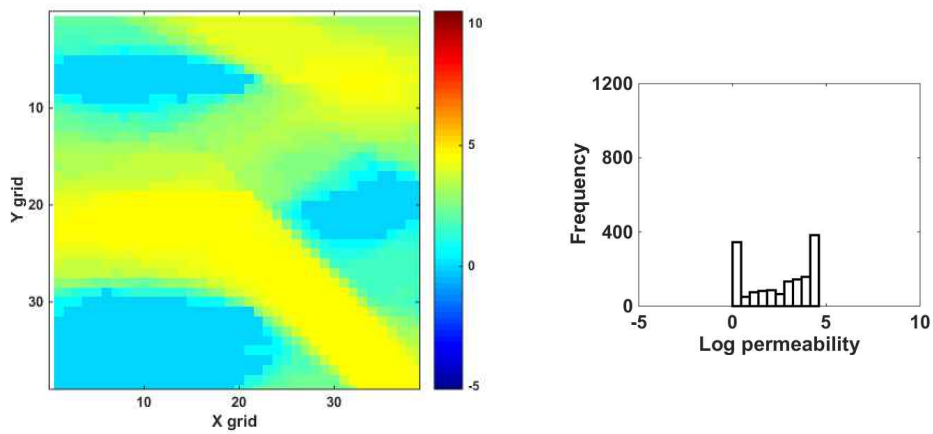

(b) Average of the initial fields

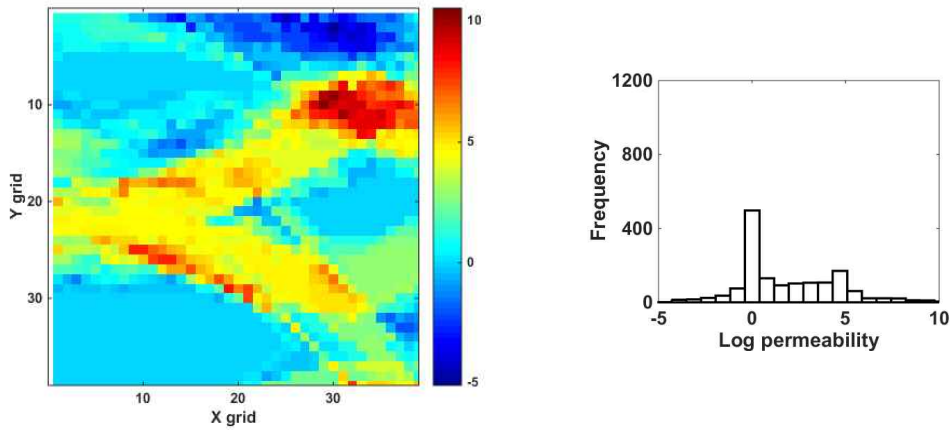

(c) EnKF alone

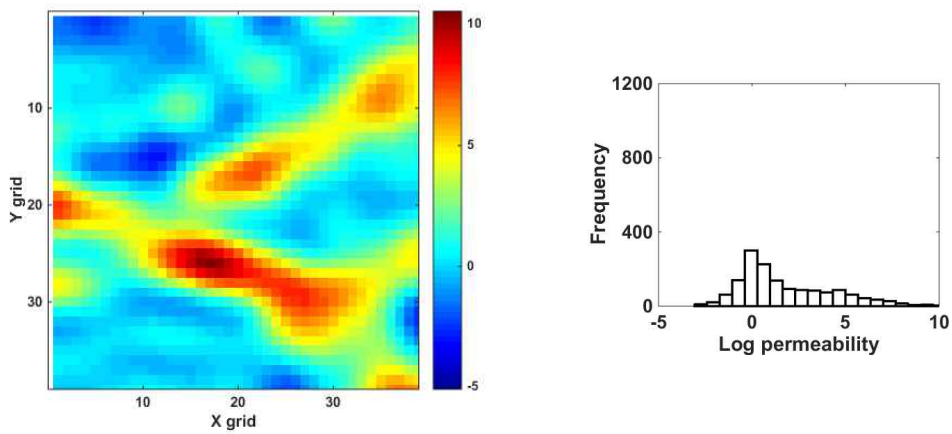

(d) EnKF with DCT

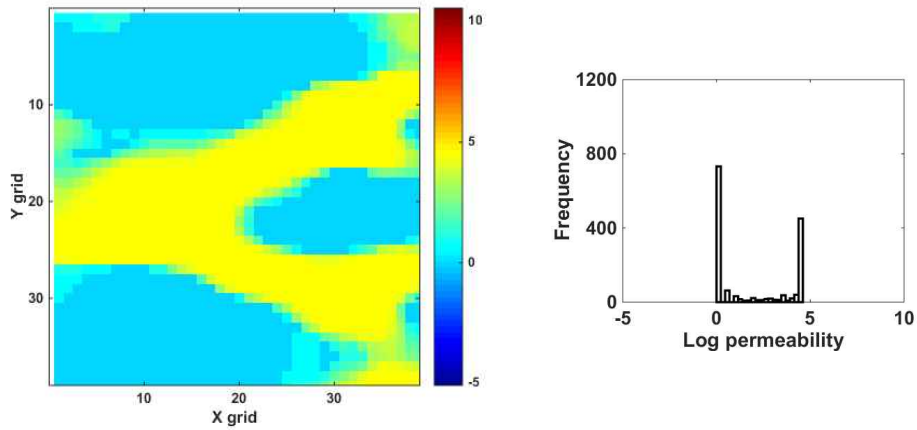

(e) The proposed method

Figure 4.7 The averages of the final assimilated log permeability fields and their histograms.

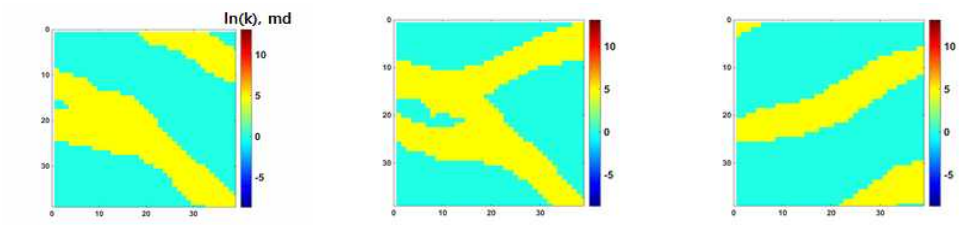

(a) The initial ensembles

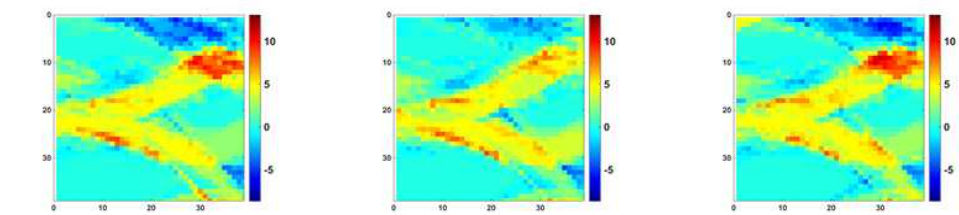

(b) EnKF

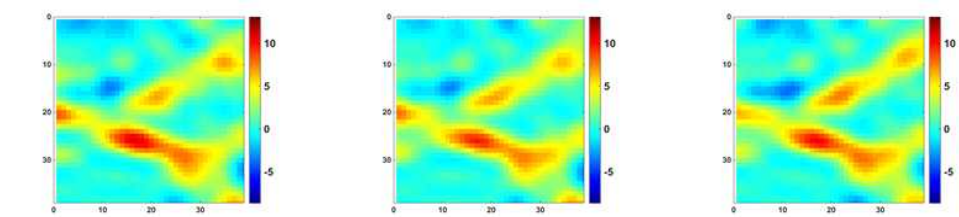

(c) EnKF with DCT

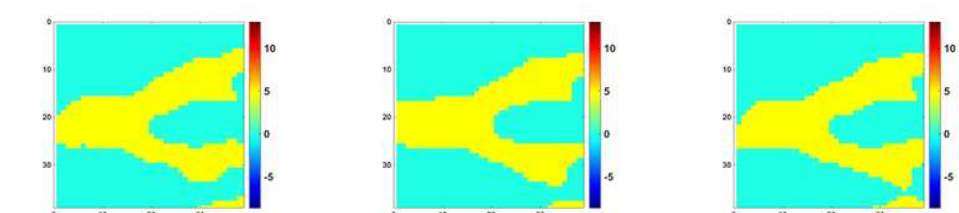

(d) EnKF with DCT and PFR

Figure 4.8 Three log permeability field examples of the initial and updated ensembles.

Table 4.3 RMSE of the averages of log-permeability fields

Cases	RMSE
Initial ensembles	2.292
Assimilated ensembles by EnKF	1.803
Assimilated ensembles by EnKF and DCT	1.853
Assimilated ensembles by the proposed method	1.537

4.5 Aquifer factors

Figure 4.9 presents characterization of the aquifer factor, MULTPV. Figure 4.9a is aquifer factor distribution of each side in the 100 initial ensemble members assigned from the uniform distribution. At the North and East sides, the averages of ensembles are smaller than the reference value. At the South and West sides, they are bigger than the reference values. Assimilated MULTPVs follow a normal distribution and present lowered uncertainty due to the characterization.

For the conventional EnKF (Figure 4.9b), the characterization results of MULTPVs are not good, especially for the North and West sides, which are overestimated. Even if DCT scheme is added to EnKF (Figure 4.9c), their estimations are not improved. This results from that DCT alone cannot estimate the true channel properties properly. It is a kind of non-uniqueness of solutions.

Only the proposed method (Figure 4.9d) characterizes MULTPVs of every side reliably. The estimated values are very similar to the reference values. These results can provide successful predictions of reservoir behaviors as shown in Figures 4.2 to 4.9 and help an operator make reasonable decisions on reservoir managements with dependable uncertainty assessments. Table 4.4 lists RMSE of MULTPVs in the three cases and RMSE of the proposed method is the lowest at 5.35.

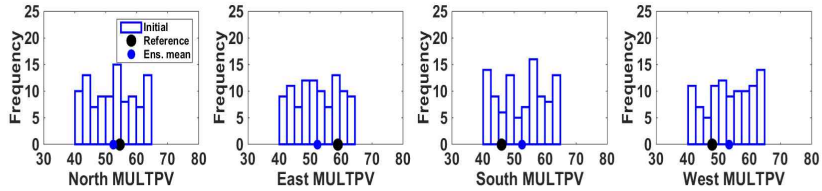

(a) Initial ensembles

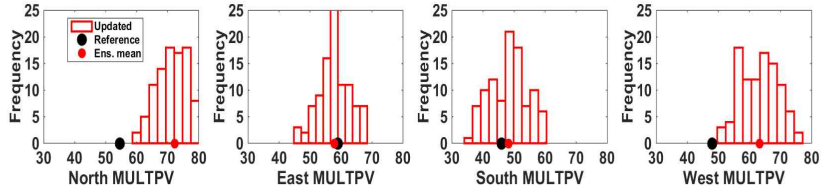

(b) EnKF alone

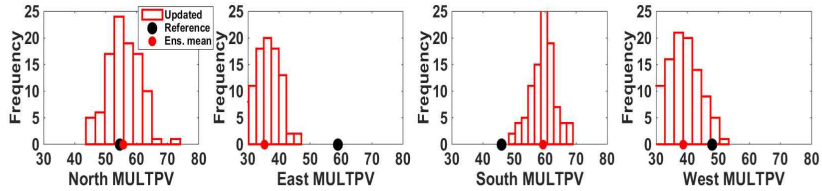

(c) EnKF with DCT

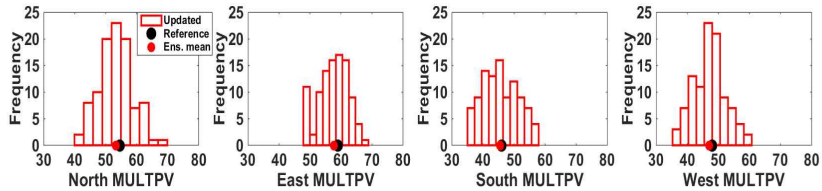

(d) The proposed method

Figure 4.9 Aquifer factor (MULTPV) of the initial and updated ensembles.

Table 4.4 RMSE of MULTPVs

Cases	RMSE
Assimilated ensembles by EnKF	11.61
Assimilated ensembles by EnKF and DCT	13.54
Assimilated ensembles by the proposed method	5.35

4.6 Comparison of characterization performances

Table 4.5 shows comparison of characterization performances of the three methods. Although the EnKF with DCT has been used to characterize channelized oil reservoirs, it cannot be applied to channelized gas reservoirs with an aquifer. The conventional EnKF may predict the gas and water production rates apparently, but channel pattern and aquifer factor cannot be estimated reliably.

Based on results analyzed in the previous sections, it is demonstrated in this study that the proposed method is a proper characterization method for channelized gas reservoirs with an aquifer. It shows the most reliable performance in predictions of channel pattern and its histogram, aquifer factors, and gas and water production rates.

Table 4.5 Comparison of performance of the three methods

Estimation or prediction	Conventional EnKF	EnKF with DCT	The proposed method
Permeability	Poor to Fair	Poor	Excellent
Aquifer factor*	Poor	Poor	Excellent
Channel pattern	Poor	Poor	Excellent
Gas production rates	Good	Poor	Good
Water production rates	Good	Poor	Excellent

*MULTPVs

5. Conclusions

Characterization of channelized gas reservoirs with an aquifer is essential to make sensible decisions due to their high uncertainty in future productions. However, the conventional EnKF or the EnKF with DCT cannot provide trustworthy performances in the prediction of channel properties and future productions because they are not able to reflect geological features of the channel properly.

The main objective of the research is to develop a methodology to estimate channel properties and aquifer strengths reliably. Since they are major sources of the uncertainty, the methodology should predict future productions properly. In this research, EnKF with DCT and PFR is proposed as a method to characterize a channelized gas reservoir with an aquifer. The proposed method has been proved as a reliable characterization method in channelized gas reservoirs with an aquifer due to its good performances in predicting channel properties, aquifer factor, and productions.

From the study, the following conclusions can be derived.

1. The conventional EnKF and EnKF with DCT cannot estimate primary properties of channel and aquifer factor reliably in channelized gas reservoirs with an aquifer. An overshooting problem is still not solved and pattern and connectivity of channel are not predicted properly. Also, the aquifer factor is over-/underestimated by the two methods. Although EnKF with DCT has been successfully used to characterize channelized oil reservoirs, it cannot be applied to channelized gas reservoirs with an aquifer.

2. PFR alleviates the overshooting issue and allows the permeability distribution to preserve the bimodal distribution. It maintains pattern and connectivity of the channel reliably. Consequently, it reduces uncertainty in

future performances by channel distribution.

3. This study has proved that the EnKF with DCT and PFR can reliably characterize aquifer factor and channel properties in channelized gas reservoirs with an aquifer using static data and production data only without any other time-lapse data. As a result, the proposed method shows consistent and reliable performances in history matching.

As further researches, the method can be modified to characterize channelized gas reservoirs with an aquifer and multiple facies. Also, stability of the proposed method in uncertainty of facies ratio should be verified. Furthermore, variations in permeability of each facies can be considered. This method may be applied to three dimensional reservoirs, various aquifer models, and real field cases with an aquifer.

References

Evensen G., 1994. Sequential data assimilation with a nonlinear quasi-geostrophic model using Monte Carlo methods to forecast error statistics. J. of geophysical research **99**(C5), 10143-10162.

Glegola M., Ditmar P., Hanea R.G., Eiken O., Vossepoel F.C., Arts R. & Klees R., 2012a. History matching time-lapse surface-gravity and well-pressure data with ensemble smoother for estimating gas field aquifer support-a 3D numerical study. SPE Journal **17**(4), 966-980.

Glegola M., Ditmar P., Hanea R.G., Vossepoel F.C., Arts R. & Klees R., 2012b. Gravimetric monitoring of water influx into a gas reservoir: a numerical study based on the ensemble Kalman filter. SPE Journal **17**(1), 163-176.

Hare J.L., Ferguson J.F., Aiken C.L.V. & Brady J.L., 1999. The 4-D microgravity method for waterflood surveillance: a model study for the Prudhoe Bay reservoir, Alaska. Geophysics **64**(1), 78-87.

Holtz M.H., 2002. Residual gas saturation to aquifer influx: a calculation method for 3-D computer reservoir model construction. Paper SPE 75502 presented at the SPE Gas Technology Symposium, Calgary, Alberta, Canada, April 30-May 2. pp. 10.

Hyne N.J., 2012. Nontechnical guide to petroleum geology, exploration, drilling, and production, second edition. Tulsa, Oklahoma: PennWell. pp. 73-84.

Jafarpour B. & McLaughlin D.B., 2007. Efficient permeability parameterization with the discrete cosine transform. Paper SPE 106453 presented at the SPE Reservoir Simulation Symposium, Houston, Texas, USA, February 26-28. pp. 9.

Jafarpour B. & McLaughlin D.B., 2008. History matching with an ensemble Kalman filter and discrete cosine parameterization. Computational geosciences **12**(2), 227-244.

Jafarpour B. & McLaughlin D.B., 2009. Reservoir characterization with the discrete cosine transform. SPE Journal **14**(1), 182-201.

Jeong H., Ki S. & Choe J., 2010. Reservoir characterization from insufficient static data using gradual deformation method with ensemble Kalman filter.Energy Sources, Part A **32**(10), 942-951.

Jung S.P. & Choe J., 2012. Reservoir characterization using a streamline-assisted ensemble Kalman filter with covariance localization. Energy Exploration & Exploitation **30**(4), 645-660.

Kim S., Lee C., Lee K., Jo K., Ryu M. & Choe J., 2015. Aquifer characterization of a gas reservoir using ensemble Kalman filter. Paper presented at the 77th EAGE Conference and Exhibition, Madrid, Spain, June 1-4. pp. 5.

Lee K., 2014. Channelized reservoir characterization using ensemble smoother with a distance-based method. PhD Thesis, Seoul National University, Seoul, South Korea.

Lee K., Jeong H., Jung S. & Choe J., 2013a. Characterization of channelized reservoir using ensemble Kalman filter with clustered covariance. Energy Exploration & Exploitation **31**(1), 17-29.

Lee K., Jeong H., Jung S. & Choe J., 2013b. Improvement of ensemble smoother with clustering covariance for channelized reservoirs. Energy Exploration & Exploitation **31**(5), 713-726.

Lee K., Jung S.P., Shin H. & Choe J., 2014. Uncertainty quantification of channelized reservoir using ensemble smoother with selective measurement data. Energy Exploration & Exploitation **32**(5), 805-816.

Lorentzen R.J., Flornes K.M. & Nævdal G., 2012. History matching channelized reservoirs using the ensemble Kalman filter. SPE Journal **17**(1), 137-152.

Nævdal G., Mannseth T. & Vefring E.H., 2002. Near-well reservoir monitoring through ensemble Kalman filter. Paper SPE 75235 presented at the SPE/DOE Improved Oil Recovery Symposium, Tulsa, Oklahoma, USA, April 13-17, 2002. pp. 9.

Nejadi S., Trivedi J. & Leung J., 2011. Improving characterization and history matching using entropy weighted ensemble Kalman filter for non-Gaussian distributions. Paper SPE 144578 presented at the SPE Western North American Regional Meeting, Anchorage, Alaska, USA, May 7-11, 2011. pp. 16,

Potter P.E., 1962. Late mississippian sandstones of Illinois. Circular 340. Urbana, Illinois: Technical Report Series, Illinois State Geological Survey.

Shin Y., Jeong H. & Choe J., 2010. Reservoir characterization using an EnKF and a non-parametric approach for highly non-Gaussian permeability fields. Energy Sources, Part A **32**(16), 1569-1578.

Stenvold T., Eiken O. & LandrØ M., 2008. Gravimetric monitoring of gas-reservoir water influx – a combined flow- and gravity-modeling approach. Geophysics **73**(6), WA123-WA131.

Yeo M., Jung S.P. & Choe J., 2014. Covariance matrix localization using drainage area in an ensemble Kalman filter. Energy Sources, Part A **36**(19), 2154-2165.

국문초록

앙상블칼만필터와 이산코사인변환을 이용한 대수층 동반 가스채널저류층의 특성화

이충호

에너지시스템공학부

서울대학교

신뢰할 수 있는 미래생산 예측과 합리적 의사결정을 위해서는 저류층 특성화를 통해 저류층특성값을 추정하는 것이 중요하다. 앙상블칼만필터(EnKF)는 저류층 특성인자를 실시간으로 교정하고 미래 생산에 대한 불확실성 평가를 제공한다.

EnKF를 이용한 채널저류층특성화는 채널의 패턴과 연결성을 파악하기 힘든 한계가 있다. 특히 대수층 동반 가스채널저류층은 이봉분포와 복잡한 채널 연결성으로 인해 유체투과율이 합리적으로 추정되기 힘들고 물의 유입으로 가스거동의 불확실성도 크다. 이로 인해 대수층 동반 가스채널저류층을 EnKF를 이용하여 성공적으로 특성화하지 못하였다.

본 논문에서는 대수층 동반 가스채널저류층의 특성화를 위해 이산코사인변환(DCT)과 암상비율보존법(PFR)을 이용한 EnKF를 제시하였다. 제안된 방법을 EnKF, DCT를 이용한 EnKF와 비교한 결과, 제안된 방법이 채널 패턴과 연결성을 가장 신뢰성 있게 추정하였다. 저류층 사면에 존재하는 대수층 인자 역시 불확실성이 줄어 합리적인 범위 내에서 예측되었다. 이 방법은 가스와 물의 미래 생산을 적절하게 예측하여 합리적인 의사결정을 도와준다.

주요어: 앙상블칼만필터, 이산코사인변환, 암상비율보존법, 가스채널저류층, 채널 패턴과 연결성, 대수층 인자

학번: 2014-20520